Explicit threshold of the toroidal ion temperature gradient mode instability

I. Sandberg[a)]
School of Electrical and Computer Engineering, Association Euratom-Hellenic Republic, National Technical University of Athens, GR-157 73 Athens, Greece

(Received 6 January 2005; accepted 3 February 2005; published online 7 April 2005)

The explicit stability threshold of the toroidal ion temperature gradient mode instability is analytically derived using the standard reactive fluid model. It is shown that in the peak density region, the threshold gets significantly smaller due to finite ion Larmor radius effects, and the marginal unstable modes acquire finite wavelengths. © *2005 American Institute of Physics*. [DOI: 10.1063/1.1883179]

Low-frequency electrostatic turbulence driven by spatial gradients is believed to be the main source of anomalous transport in magnetically confined fusion plasmas.[1,2] During the last years, a significant number of both theoretical and numerical investigations in plasma dynamics has been focused on the effects related with the development of the ion temperature gradient (ITG) mode instability.[3] This is due to the successful interpretations of various experimental trends—related to the observed levels of turbulent transport in tokamak plasmas—which are based on the dynamics of the ITG mode instability.[4]

The derivation of a general ITG model can be obtained either from a low-frequency expansion of the general fluid equations[5] based on the drift velocity ordering, or by using as a starting point the nonlinear gyrokinetic equation as in Ref. 6. For the development of the ITG instability, the ion temperature gradient is necessary to be combined with other effects. The magnetic curvature, the parallel incompressibility, or the presence of impurity species[7] are main examples of such additional effects.

However, in a toroidal system the instability is mainly driven by the magnetic field curvature[8] and it is termed toroidal ITG mode instability. The associated marginal instability threshold has been determined and analyzed in numerous works and in a variety of interacting physical processes, such as negative magnetic shear, electron trapping, or ion Landau damping. For instance, we may refer to the analysis based on the advanced fluid model[9]—in Ref. 10 or more recently in Ref. 11. However, to our knowledge, the relevant investigations have derived the marginal stability threshold without taking explicitly into account the finite ion Larmor radius (FLR) effects. As a result, the derived thresholds either depend on the wave numbers of the marginally unstable modes, or correspond—as we will show here—to larger values than the actual instability threshold. The resulting inaccuracy is reflected on the asymptotic behavior of the conventional stability curve $\eta_i(\epsilon_n,\tau)\to\infty$ when $\tau\epsilon_n\to 0$ (e.g., Ref. 9, p. 125).

In what follows, the standard advanced reactive fluid model by Weiland[9] is adopted and the linear stability properties of the toroidal ITG driven modes are investigated by keeping rigorously the FLR terms. Effects attributed to parallel ion dynamics, magnetic shear, electron particle trapping, Landau damping, or finite β effects are omitted. By using a low-frequency expansion based on the standard drift velocity ordering, the ion continuity and the ion temperature equations, which describe the dynamics of the ITG modes, can be written in the following normalized form,[12] respectively:

$$\frac{\partial n_i}{\partial t}-\left[\frac{\partial}{\partial t}-\tau(1+\eta_i)\frac{\partial}{\partial y}\right]\nabla_\perp^2\phi+\frac{\partial\phi}{\partial y}-\epsilon_n\frac{\partial}{\partial y}[\phi+\tau(n_i+T_i)]=\{\phi,\nabla_\perp^2\phi-n_i+\tau\nabla_\perp^2(n_i+T_i)\} \tag{1}$$

and

$$\frac{\partial T_i}{\partial t}-\frac{5}{3}\tau\epsilon_n\frac{\partial T_i}{\partial y}+\left(\eta_i-\frac{2}{3}\right)\frac{\partial\phi}{\partial y}-\frac{2}{3}\frac{\partial n_i}{\partial t}=\left\{\phi,\frac{2}{3}n_i-T_i\right\}. \tag{2}$$

The curly brackets in the right-hand side of Eqs. (1) and (2) denote the Poisson bracket defined by $\{A,B\}=\partial_x A\partial_y B-\partial_x B\partial_y A$. Details on the derivation of these equations may be found in Ref. 9. The length and the time scales have been normalized with respect to $\rho_s=c_s/\omega_{ci}$ and L_n/c_s, respectively, where $c_s^2=T_e/m_i$ is the ion sound velocity defined at electron temperature, $\omega_{ci}=eB_0/m_ic$ is the ion gyrofrequency, and $L_g^{-1}=-d\ln g(r)/dr$ describes the inverse characteristic scale length of inhomogeneity, along the radial direction, of the plasma parameter $g(r)$. The electrostatic potential has been normalized by $\phi=e\delta\phi/T_eL_n/\rho_s$, the perturbed density by $n=\delta n/n_0L_n\rho_s$, and the perturbed ion temperature by $T_i=\delta T_i/T_{i0}L_n/\rho_s$. Furthermore, the curvature of the magnetic field lines R and the ion temperature inhomogeneity scale length L_{T_i} are given in terms of the plasma inhomogeneity scale length L_n by $\epsilon_n=2L_n/R$ and $n_i=L_n/L_{T_i}$, respectively. Furthermore, τ denotes the ratio of ion to electron temperature, $\tau=T_i/T_e$.

Considering quasineutral oscillations and assuming Boltzmann distribution for the electron density response, i.e., $n_e=n_i=\phi$, we linearize Eqs. (1) and (2) and by applying the usual Fourier expansion for the perturbed quantities, i.e, $\tilde{g}(r,t)=\tilde{g}\exp(i\mathbf{k}_\perp\cdot\mathbf{r}-i\omega t)$, the dispersion relation for the toroidal ITG modes is derived. Here, $\mathbf{k}_\perp$ denotes the wave vector perpendicular to the toroidal axis of the magnetic field and ω the frequency of the toroidal ITG mode. The solution

a)Electronic mail: sandberg@central.ntua.gr

of the dispersion relation leads to the determination of the real frequency ω_r and the growth rate γ_k of the mode, which are given by

$$\omega_r = \frac{k_y}{2(1+k_\perp^2)}\left\{1-\epsilon_n-\frac{10}{3}\epsilon_n\tau-\left[\tau(1+\eta_i)+\frac{5}{3}\tau\epsilon_n\right]k_\perp^2\right\} \tag{3}$$

and

$$\gamma_k = \frac{k_y}{2(1+k_\perp^2)}\sqrt{f(k_\perp^2)}, \tag{4}$$

respectively. The polynomial $f(k_\perp^2)$ under the square root of Eq. (4) can be written in the following suitable form:

$$f(k_\perp^2) = -\tau^2\left(1+\eta_i-\tfrac{5}{3}\epsilon_n\right)^2k_\perp^4+2\tau(1+\epsilon_n)(\eta_i-\eta_B)k_\perp^2 + 4\epsilon_n\tau(\eta_i-\eta_C). \tag{5}$$

The parameters η_B and η_C are given by

$$\eta_B = \frac{4\epsilon_n-1}{\epsilon_n+1}-\frac{5}{3}\frac{\epsilon_n^2}{\epsilon_n+1}\left(1-\frac{4}{3}\tau\right) \tag{6}$$

and

$$\eta_C = \frac{2}{3}+\frac{10}{9}\epsilon_n\tau+\frac{(\epsilon_n-1)^2}{4\epsilon_n\tau}. \tag{7}$$

The development of the toroidal ITG instability requires the condition $f(k_\perp^2)>0$ to be hold. As a consequence, unstable modes will be those with perpendicular wave number in the range defined by the roots of equation $f(k_\perp^2)=0$, which are given by

$$k_{\perp\pm}^2 = \frac{(\epsilon_n+1)(\eta_i-\eta_B)\pm\sqrt{D_\eta}}{\tau\left(1+\eta_i-\frac{5}{3}\epsilon_n\right)^2}, \tag{8}$$

where

$$D_\eta = (1+\epsilon_n)^2(\eta_i-\eta_B)^2+4\epsilon_n\tau(\eta_i-\eta_C)\left(1+\eta_i-\tfrac{5}{3}\epsilon_n\right)^2. \tag{9}$$

A sufficient condition for the development of the instability is these roots to be real and at least one of them to be positive. Inspection of Eqs. (8) and (9) leads us to the conclusion that for $\eta_i<\eta_B,\eta_C$ the toroidal ITG instability cannot take place since $k_{\perp\pm}^2<0$. On the other hand, instability certainly occurs when the condition $\eta_i>\eta_C$ holds, independently on the value of η_B. In this case, it is $k_{\perp-}^2<0$, and consequently the wave numbers of the unstable toroidal ITG modes range as $0<k_\perp^2<k_{\perp+}^2$. The value η_C is the conventional threshold of the toroidal ITG instability[11,12] obtained from Eq. (5) in the limit of negligible FLR effects. However, when FLR effects are taken into account, η_C becomes the marginal stability threshold *only* when $\eta_C<\eta_B$, and the marginal unstable mode has wave number $k_\perp=0$. In the opposite case, i.e., when $\eta_B<\eta_C$, the threshold η_{th} is expected to be $\eta_B<\eta_{th}<\eta_C$.

Before we proceed with the determination of η_{th}, we first investigate under which conditions the relation $\eta_C>\eta_B$ holds. Thus, we need to express the difference $\eta_C-\eta_B$ as follows:

$$\eta_C-\eta_B = \frac{(\epsilon_n-1)^2}{4\epsilon_n\tau}-\frac{10\epsilon_n}{9}\frac{\epsilon_n-1}{\epsilon_n+1}\left[\tau-\frac{3}{2}\left(1-\frac{1}{\epsilon_n}\right)\right].$$

For $\epsilon_n<1$, it is $\eta_C>\eta_B$ for any τ. The same inequality is valid also for $\epsilon_n>1$ when τ belongs to the interval $0<\tau<\tau_{CB}(\epsilon_n)$. The parameter $\tau_{CB}(\epsilon_n)$ is given by $\tau_{CB}(\epsilon_n)=3[\epsilon_n-1+\sqrt{(\epsilon_n-1)(7\epsilon_n-3)/5}]/4\epsilon_n$, and defines a curve where $\eta_C=\eta_B$. It is evident now that η_C is the actual marginal stability threshold *only when* $\epsilon_n>1$ *and* $\tau>\tau_{CB}$.

In what follows, we limit our analysis in the case $\eta_C>\eta_B$ and we seek for a threshold in the range $\eta_B<\eta_{th}<\eta_C$. Since necessary condition for the existence of the toroidal ITG instability is $D_\eta>0$, the roots of equation $D_\eta=0$ are appropriate candidates for the threshold. These are

$$\eta_* = \tfrac{10}{9}\epsilon_n\tau+\tfrac{2}{3}, \tag{10}$$

$$\eta_\pm = \frac{5}{3}\epsilon_n-1-\frac{1}{2\tau}\pm\sqrt{\frac{10}{9}\epsilon_n^2+\frac{1}{4\tau^2}+\frac{5}{3}\frac{\epsilon_n}{\tau}(1-\epsilon_n)}. \tag{11}$$

A rigorous analysis of Eqs. (6), (7), (10), and (11) shows that in the range of present interest, i.e., $\eta_C>\eta_B$, the derived roots η_*, $\eta_\pm$ obey the following ordering:

$\eta_-<\eta_+<\eta_B<\eta_*$ when $\epsilon_n<1$ for any τ,

$\eta_-<\eta_+<\eta_B<\eta_*$ when $\epsilon_n>1$ for $\tau<\tau_*(\epsilon_n)$,

$\eta_-<\eta_*<\eta_B<\eta_+$ when $\epsilon_n>1$ for $\tau_*(\epsilon_n)<\tau<\tau_{CB}(\epsilon_n)$.

The parameter $\tau_*(\epsilon_n)$ is given by $\tau_*(\epsilon_n)=3(1-1/\epsilon_n)/2$, and defines a curve where $\eta_*(\epsilon_n,\tau_*)=\eta_+(\epsilon_n,\tau_*)=\eta_B(\epsilon_n,\tau_*)$. From the analysis above, we conclude that the explicit threshold of the toroidal ITG instability is given by

$$\eta_{th}(\epsilon_n,\tau) = \begin{cases} \eta_* \text{ for } \epsilon_n<1, \\ \eta_* \text{ for } \epsilon_n>1 \quad \text{when } 0<\tau<\tau_*, \\ \eta_+ \text{ for } \epsilon_n>1 \quad \text{when } \tau_*<\tau<\tau_{CB}, \\ \eta_C \text{ for } \epsilon_n>1 \quad \text{when } \tau>\tau_{CB}. \end{cases} \tag{12}$$

It is evident that FLR effects are destabilizing for values of ϵ_n smaller than unity, and reduce slightly the threshold in the flat density regime. These results are in qualitative agreement with the Nyquist analysis of the full gyrokinetic dispersion relation in Ref. 6, where the authors claimed that critical condition for the instability to take place is $\eta_i>2/3$.

The threshold value η_* is similar to that derived by applying the necessary (but not sufficient) condition $\gamma_k=0$ in a three pole reactive model in Refs. 9 and 11. The authors claimed that the growth for $\eta_i<\eta_C$ is attributed to the parallel dynamics. However, a careful inspection of Ref. 11 leads to the conclusion that the particular derivation is possible only for finite values of the FLR terms. In view of the present results—where ion parallel dynamics is excluded—it

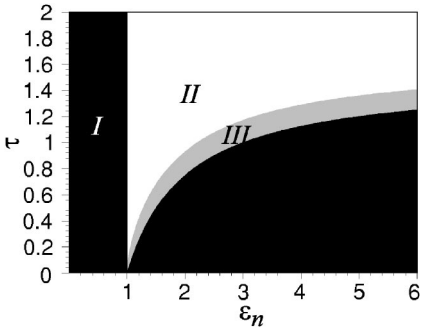

FIG. 1. Instability thresholds in the plane (ϵ_n, τ). The exact marginal stability threshold is given by $\eta_*(\epsilon_n, \tau)$ in the black regions, by $\eta_C(\epsilon_n, \tau)$ in the white region, and by $\eta_+(\epsilon_n, \tau)$ in the gray one.

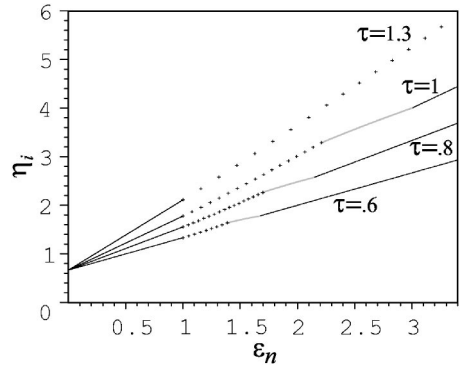

FIG. 2. Marginal stability curves $\eta_i(\epsilon_n)$ for different values of τ. The black solid parts of each curve corresponds to η_* (region I in Fig. 1), the dotted parts to η_C (region II in Fig. 1), and the gray solid parts to η_+ (region III in Fig. 1).

becomes clear that the growth for $\eta_i < \eta_C$ is attributed to the FLR effects and not to the parallel compressibility, as was erroneously considered so far.[9,11]

By substituting ϵ_n with $g\epsilon_n$,[12] and η_{th} by $\eta_{th}/(1-f_e)$,[10] one may obtain the corresponding thresholds from Eq. (12) for the cases of elongated flux surfaces and trapped electrons, respectively. Here, g denotes the geometrical factor in the ratio between curvature and diamagnetic drift velocities, i.e., $g\epsilon_n = \omega_D/\omega_*$, due to the elongated flux surfaces and f_e the fraction of the trapped electron population.

In Fig. 1, we depict the areas of the plane (ϵ_n, τ) where the different expressions for the threshold are applicable, according to Eq. (12). In region I ($\epsilon_n < 1$ and $\epsilon_n > 1$ with $\tau < \tau_+$) the threshold is η_*, in region II ($\epsilon_n > 1$ with $\tau > \tau_{CB}$) it is η_C, and in region III ($\epsilon_n > 1$ with $\tau_+ < \tau < \tau_{CB}$) it is η_+. In Fig. 2 we present the marginal stability curve $\eta_{th}(\epsilon_n)$ for different values of τ. The stability diagram shows the trend for increasing deviation from marginal stability as we move towards the edge. In order to stress the contribution of the FLR effects, we present in Fig. 3 the stability curves $\eta_{th}(\epsilon_n)$ and $\eta_{th}(\tau)$ in comparison with the conventional threshold—derived in the absence of FLR effects—which behaves asymptotically $\eta_C(\epsilon_n, \tau) \to \infty$ as $\tau\epsilon_n \to 0$. It is evident that for small values of τ and ϵ_n, the stability threshold gets significantly smaller compared to η_C. In Fig. 4 the normalized growth rate of the unstable ITG modes given by Eq. (4) is depicted versus $k_\perp^2$ (a) and versus ϵ_n (b) for different values of ϵ_n and $k_\perp$, respectively, and for η_i slightly above the stability threshold. It is evident that the unstable modes acquire finite wavelengths for $\eta_i < \eta_C$, while FLR effects stabilize the large wavelength modes, i.e., those in the range $0 < k_\perp < k_-$.

Furthermore, there always exist a critical wave number $k_{\perp m}$ where a maximum growth occurs for given conditions. This wave number can be determined by the condition $d\gamma_k/dk_\perp^2 = 0$, which leads to the following cubic equation:

$$f(k_{\perp m}^2)\frac{k_{\perp m}^2 - 1}{k_{\perp m}^2 + 1} + 2\tau k_{\perp m}^2 \left[\tau\left(1 + \eta_i - \frac{5}{3}\epsilon_n\right)^2 k_{\perp m}^2 + (1 + \epsilon_n)(\eta_B - \eta_i) \right] = 0. \tag{13}$$

Close to the marginal stability conditions, i.e., $f(k_{\perp m}^2) \simeq 0$, Eq. (13) can be approximately solved giving the following solutions:

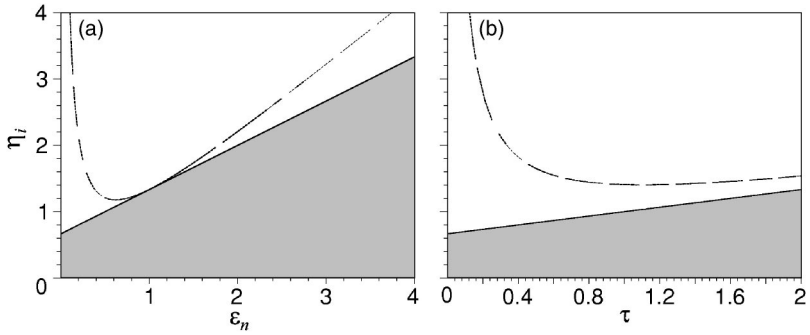

FIG. 3. The marginal stability curve η_i: (a) vs ϵ_n, for $\tau = 0.6$ and (b) vs τ, for $\epsilon_n = 0.3$. The white and the gray areas denote the unstable and stable regions, respectively, as defined by the exact threshold. The dashed line represents the threshold η_C which is valid in absence of FLR effects.

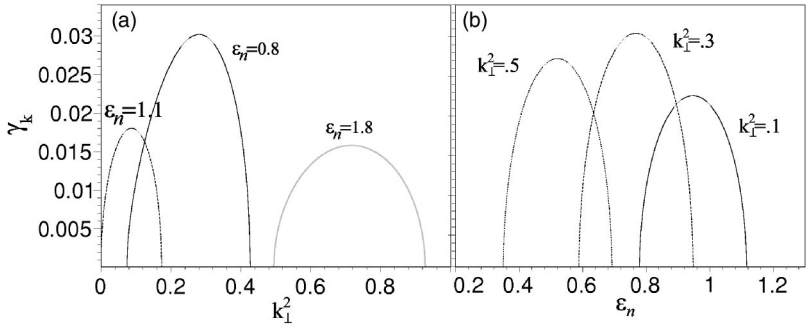

FIG. 4. The normalized growth rate γ_k of the toroidal ITG instability for purely poloidal propagation ($k_x=0$) and $\tau=0.8$: (a) vs $k_\perp^2$, for (i) $\epsilon_n=0.8$, $\eta_i=1.005\eta_*$ (region I in Fig. 1), (ii) $\epsilon_n=1.1$, $\eta_i=1.005\eta_C$ (region II in Fig. 1), and (iii) $\epsilon_n=1.8$, $\eta_i=1.0002\eta_+$ (region III in Fig. 1); (b) vs ϵ_n for three distinct ITG modes; $k_\perp^2=0.1$, 0.3, and 0.5 for $n_i=1.005\eta_*$.

$$k_{\perp m}^2 \simeq \begin{cases} \dfrac{(1+\epsilon_n)(\eta_i-\eta_B)}{\tau\left(1+\eta_i-\dfrac{5}{3}\epsilon_n\right)^2} \\ \dfrac{2}{3}\dfrac{\eta_i-\eta_B+\epsilon_n(\eta_C-\eta_B)-\sqrt{[\eta_i-\eta_B+\epsilon_n(\eta_C-\eta_B)]^2-3\tau\left(1+\eta_i-\dfrac{5}{3}\epsilon_n\right)^2}}{\tau\left(1+\eta_i-\dfrac{5}{3}\epsilon_n\right)^2}. \end{cases} \tag{14}$$

These expressions are in excellent agreement with the wave numbers of the most unstable modes in Fig. 4(a). The first solution corresponds to the wave number of the most unstable mode when $\eta_B<\eta_{th}\simeq\eta_i<\eta_C$ (regions I and III in Fig. 1) and corresponds to the marginal unstable mode given by Eq. (8) for $D_\eta=0$. The second solution is valid for $k_\perp^2 \ll 1$, corresponds to the wave number of the most unstable mode when $\eta_i\simeq\eta_{th}=\eta_C<\eta_B$ (region II in Fig. 1) and becomes equal to zero for $\eta_i=\eta_{th}=\eta_C$ as expected.

In this work, the explicit marginal stability threshold for the development of the toroidal ITG instability was derived in the frame of the standard advanced reactive fluid model. It was shown that FLR effects can decrease significantly the marginal instability threshold. These results predict that a significant activity of toroidal ITG turbulence can be present at regions of peaked plasma density, such as the plasma edge, modifying the confinement in the hot ion mode regime of tokamak operation. Furthermore, it was shown that toroidal ITG modes may acquire finite wavelengths as they deviate from stability. It is worthwhile to mention here that these consequences can be rather crucial regarding the properties of the large scale flows that are attributed to the development of the toroidal ITG instability near marginal conditions.

ACKNOWLEDGMENTS

The author is grateful to Professor V. P. Pavlenko for useful discussions on the topic. Part of this work was conducted during a visit of the author to the Department of Astronomy and Space Physics at the Uppsala University. The hospitality of that department is greatly appreciated. This work was supported under the Contract of Association (Contract No. ERB 5005 CT 99 0100) between the European Atomic Energy Community and the Hellenic Republic. The sponsors do not bear any responsibility for the contents in this work.

[1] W. Horton, Rev. Mod. Phys. **71**, 735 (1999).
[2] P. W. Terry, Rev. Mod. Phys. **72**, 109 (2000).
[3] L. I. Rudakov and R. Z. Sagdeev, Sov. Phys. Dokl. **6**, 415 (1961).
[4] X. Garbet *et al.*, Plasma Phys. Controlled Fusion **46**, 557 (2004).
[5] S. I. Braginskii, in *Reviews of Plasma Physics*, edited by M. A. Leontovich (Consultants Bureau, New York, 1965), Vol. 1.
[6] H. Biglari, P. H. Diamond, and M. N. Rosenbluth, Phys. Fluids B **1**, 109 (1989).
[7] D. Jovanović and W. Horton, Phys. Plasmas **2**, 1561 (1995).
[8] B. Coppi and F. Pegoraro, Nucl. Fusion **17**, 969 (1977).
[9] J. Weiland, *Collective Modes in Inhomogeneous Plasmas* (IOP, Bristol, 2000).
[10] A. Jarmén, P. Andersson, and J. Weiland, Nucl. Fusion **27**, 941 (1987).
[11] S. C. Guo and J. Weiland, Nucl. Fusion **37**, 1095 (1997).
[12] J. Anderson, H. Norman, R. Singh, and J. Weiland, Phys. Plasmas **9**, 4500 (2002).